Annals of Botany **91**: 771–781, 2003
doi:10.1093/aob/mcg080, available online at www.aob.oupjournals.org

A Coupled Model of Photosynthesis, Stomatal Conductance and Transpiration for a Rose Leaf (*Rosa hybrida* L.)

SOO-HYUNG KIM† and J. HEINRICH LIETH*
Environmental Horticulture, University of California, Davis, CA 95616, USA

Received: 20 November 2002 Returned for revision: 6 January 2003 Accepted: 3 February 2003 Published electronically: 27 March 2003

The following three models were combined to predict simultaneously photosynthesis, stomatal conductance, transpiration and leaf temperature of a rose leaf: the biochemical model of photosynthesis of Farquhar, von Caemmerer and Berry (1980, *Planta* **149**: 78–90), the stomatal conductance model of Ball, Woodrow and Berry (In: Biggens J, ed. *Progress in photosynthesis research*. The Netherlands: Martinus Nijhoff Publishers), and an energy balance model. The photosynthetic parameters: maximum carboxylation rate, potential rate of electron transport and rate of triose phosphate utilization, and their temperature dependence were determined using gas exchange data of fully expanded, young, sunlit leaves. The stomatal conductance model was calibrated independently. Prediction of net photosynthesis by the coupled model agreed well with the validation data, but the model tended to underestimate rates of stomatal conductance and transpiration. The coupled model developed in this study can be used to assist growers making environmental control decisions in glasshouse production.

Key words: *Rosa hybrida* L., photosynthesis, stomatal conductance, transpiration, coupled model, cut-flower, crop simulation, calibration, validation.

INTRODUCTION

Crop simulation models are invaluable tools for optimization of the glasshouse microclimate and for making cultural decisions for increasing production and profit of glasshouse crops, including cut-flower roses. As one of the most important modules of such crop simulation models, a photosynthesis model should be comprehensive, encompassing all of the major variables that can be controlled and/or monitored using the environmental control system in the glasshouse. This raises the need for a mechanistic model of photosynthesis. The biochemical model of photosynthesis for C_3 leaves by Farquhar, von Caemmerer and Berry (FvCB model) (Farquhar *et al*., 1980) has been adopted extensively in studies of ecological and physiological modelling, including studies on the effect of elevated CO_2 on plant productivity (Medlyn *et al*., 1999). A major advantage of using the biochemical model is that it is mechanistic and, therefore, capable of describing underlying processes that might not be well described by simple empirical approaches. The disadvantage of the model has been that it requires rather extensive calibration of a number of parameters (Wullschleger, 1993; Cannell and Thornley, 1998). Application of the biochemical model in crop simulation models for agricultural or horticultural purposes has been limited due to the complex parameterization procedure. Fortunately, recent development of highly sophisticated gas-exchange systems has made the process of estimating model parameters easier. Also, the number of parameters to be fitted can be reduced by assuming that some are invariant across species of C_3 plants.

Estimation of substomatal CO_2 partial pressure (C_i) from given atmospheric CO_2 (C_a) is critical for practical use of the model because the FvCB model operates using C_i instead of C_a. C_i may be estimated to be proportional to C_a under certain conditions. The ratio of C_i/C_a is assumed to be constant (0·7–0·8) in some studies owing to the complexity of C_i estimation. However, use of the fixed C_i/C_a ratio may not be appropriate for dynamic crop simulation models, as they should cover a variety of conditions where a fixed ratio may not be valid. To be useful in predicting gas exchange responses to varying environmental conditions, a photosynthesis model should be integrated with a model describing stomatal conductance (g_s) so as to obtain realistic estimates of C_i. This allows a coupling of the supply function of diffusion through the stomata to the demand function of the CO_2 fixation reaction.

A coupled approach to photosynthesis–stomatal conductance–transpiration modelling has been proposed (Collatz *et al*., 1991; Harley *et al*., 1992; Leuning *et al*., 1995; Nikolov *et al*., 1995) that combines the FvCB photosynthesis model with a model of stomatal conductance (Ball *et al*., 1987; Leuning, 1995) and an energy budget equation. This coupled-model approach can describe the photosynthetic behaviour of leaves by taking into account the biochemical limitation for CO_2 (demand) as well as the stomatal limitation to supply of CO_2. Sharkey (1985) included the rate of triose phosphate utilization (TPU) as one of the important biochemical limitations in photosynthesis. Harley *et al*. (1992) implemented the TPU limitation in their model.

* For correspondence. Fax +1 (530) 752 1819, e-mail jhlieth@ucdavis.edu
† Present address: Alternate Crops and Systems Laboratory,USDA-ARS, Bldg. 001 Rm 342, BARC-W, Beltsville, MD 20705, USA.

A model for photosynthesis of rose leaves as a function of photosynthetically active radiation (PAR), leaf temperature and leaf age was previously developed for the rose variety Cara Mia (Lieth and Pasian, 1990). The model did not include CO_2 as a driving variable. The FvCB model has been used to study the photosynthetic properties of rose canopy (Gonzalez-Real and Baille, 2000). Coupled gas exchange models have rarely been developed for horticultural and/or ornamental crops such as roses.

The objective of this study was to formulate and test a coupled model of photosynthesis, stomatal conductance and transpiration for rose by combining widely accepted sub-models. The coupled model is to be used as a module in a rose crop simulation model.

MODEL DESCRIPTION

Photosynthesis, stomatal conductance and energy balance sub-models

The models are summarized in the Appendix, and parameters and variables listed. The biochemical model for C_3 photosynthesis by Farquhar *et al*. (1980) was used as modified by Harley *et al*. (1992) and de Pury and Farquhar (1997). The parameters of photosynthetic capacity: maximum carboxylation rate (V_{cmax}), potential rate of electron transport (J_{max}) and rate of triose phosphate utilization (P_u) were modelled to account for the effect of leaf age, assuming that all three parameters are dependent on leaf age to the same extent [eqn (A10)].

The stomatal conductance model [eqn (A11)] proposed by Ball, Woodrow and Berry (BWB model) (Ball *et al*., 1987) was calibrated and tested for rose leaves. Humidity at the leaf surface (h_s) was obtained by applying a quadratic equation [eqn (A16)]. The energy balance equation was used to estimate leaf temperature (T_L) as a function of stomatal conductance (g_s), boundary layer conductance (g_b) and the environmental variables: air temperature, absorbed long-wave and short-wave radiation, and relative humidity (Campbell and Norman, 1998). The leaf temperature was determined iteratively using a linear solution of the energy budget equation [eqn (A18)] using the Newton–Raphson method. Assuming that the water vapour pressure inside the leaf is the same as saturation vapour pressure (e_s) at the leaf temperature, the rate of transpiration was calculated using the diffusion equation [eqn (A23)].

Coupling the models

The FvCB model uses C_i [eqns (A2) and (A3)] and T_L [eqns (A7)–(A9)], among others, as driving variables. The BWB model requires the net photosynthetic rate (A) as an input [eqn (A11)], while C_i results from the interaction of A and g_s [eqn (A24)]. T_L is estimated iteratively from a linear solution of the energy budget equation [eqn (A18)] using air temperature (T_a), and the conductances for heat (g_h) and water vapour (g_v) as input variables. The diffusion equation is used to relate C_a, C_s and C_i using A, g_s and g_b [eqns (A13) and (A24)]. Therefore, the three sub-models (FvCB, BWB and energy balance) are interdependent. A nested iterative procedure was used to solve this relation numerically (Fig. 1). Initially, T_L and C_i were assumed to be equal to T_a and $0{\cdot}7C_a$, respectively, so as to obtain an estimate of A, which was then used to obtain g_s. C_i was estimated using the resulting A and g_s [eqn (A24)]. This process was solved iteratively using the Newton–Raphson method until C_i was stable. Subsequently, T_L was computed using T_a and g_s [eqn (A18)] and compared with the initial T_L. When the new T_L agreed to within 0·001 °C with the initial T_L, the iteration was assumed to have converged.

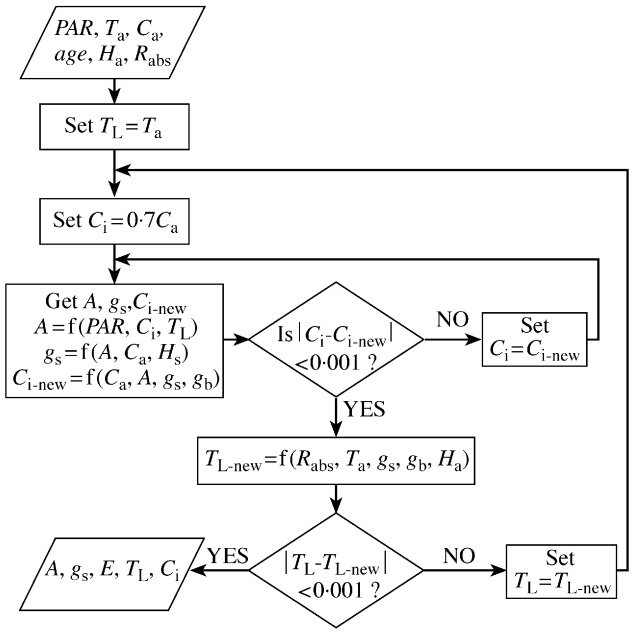

FIG. 1. Schematic diagram of the model flow.

MATERIALS AND METHODS

Plant material

Fifteen rose plants (*Rosa hybrida* L. 'Kardinal') grafted onto 'Natal Brier' rootstock and transplanted into 13 l pots in May 1997 were used for the leaf photosynthesis measurements for calibration and validation of the model. A potting mix containing sand, redwood sawdust, and peat moss (1 : 1 : 1, v/v) was used as growing medium. Tensiometer-based irrigation was used to control root-zone moisture tension, with set-points of 1·0 and 3·0 kPa (Oki *et al*., 2001), delivering a modified half-strength Hoagland's solution. Plants were grown in the glasshouse at the Department of Environmental Horticulture at the University of California (Davis, USA). Air temperature set-points inside the glasshouse were 24/20 °C day/night.

Gas exchange measurements

A photosynthesis system (LI-6400; LI-COR, Lincoln, NE, USA) with a red/blue LED light source (LI6400-02B) mounted onto a 6-cm^2 clamp-on leaf chamber was used to determine light and A/C_i responses under various environ-

mental conditions. Terminal leaflets of randomly selected, fully developed, young sunlit leaves (approx. 20 d from unfolding) of the flowering shoots (developed between September and November 2000) were used. For generation of A/C_i and light response curves, an automated protocol built into LI-6400 was used. The programme was configured to advance to the next step if the sum of the three coefficients of variation (CO_2, water vapour and flow rate) was less than 0·3 %, with minimum wait time of 3 min. Each leaf was equilibrated to the initial conditions by waiting at least 5 min before executing the automated protocol. The photosynthetic response to C_i of 15 individual leaves was measured at 0, 50, 100, 200, 300, 400, 600, 800, 1200 and 1500 μmol mol^{-1} CO_2 at 1500 μmol m^{-2} s^{-1} of incident PAR at a leaf temperature of 25 °C and relative humidity (h_a) of approx. 50 %. A/C_i response measurements were started at ambient conditions, decreased to nearly the compensation point, returned to ambient, and then increased to higher concentrations to ensure that the stomata stayed open throughout the measurements. The light response of nine leaves was determined at several PAR levels between 0 and 2000 μmol m^{-2} s^{-1} at 25 °C leaf temperature and 350 μmol mol^{-1} CO_2 inside the leaf chamber. For light response curves, measurements started with a leaf equilibrated to high light and the light level was then gradually decreased.

The A/C_i response of a total of 54 leaves was investigated at various leaf temperatures (10, 15, 20, 25, 30, 35 and 40 °C) to determine the temperature dependence of the photosynthetic parameters. The photosynthesis system (LI-6400) was able to control the leaf temperatures between 20 and 30 °C under growing conditions in the glasshouse. Growth chambers were used to provide conditions resulting in leaf temperatures below 20 °C or above 30 °C. Whenever a growth chamber was used, plants were moved into it at least 2 h before measurements to allow them time to acclimate.

Using 21 leaves, the response of g_s to relative humidity (0·05–0·90), PAR (>100 μmol m^{-2} s^{-1}), leaf temperature (10–40 °C) and a range of CO_2 levels (>50 μmol mol^{-1}) was determined to calibrate the stomatal conductance model. Relative humidity was controlled either by using the bypass valve on the desiccant tube containing anhydrous calcium carbonate (Drierite; W.A. Hammond Drierite Company, Ltd, Xenia, OH, USA), or by adjusting the flow rate of air through the leaf chamber. Measurements used to calibrate the stomatal conductance model were collected by waiting until the rates of C_i, transpiration and CO_2 assimilation had stabilized before taking readings; this wait-time ranged from 5 to 30 min depending on the leaves and the environmental conditions of the chamber.

The dependence of the model on leaf age was calibrated using a separate data set collected in 1999. Leaf gas exchange measurements were made using a CIRAS-1 photosynthesis system (PP Systems, Hitchin, UK) between May and October 1999. The date on which 130 individual leaves unfolded was noted throughout the season, and the age of the leaves used for calibration was determined in 'days after unfolding'. Measurements for characterizing leaf age effects were made in sunlight (>900 μmol m^{-2} s^{-1}) at ambient CO_2 (340–370 μmol mol^{-1}) and growth temperature (24–27 °C) conditions in the glasshouse.

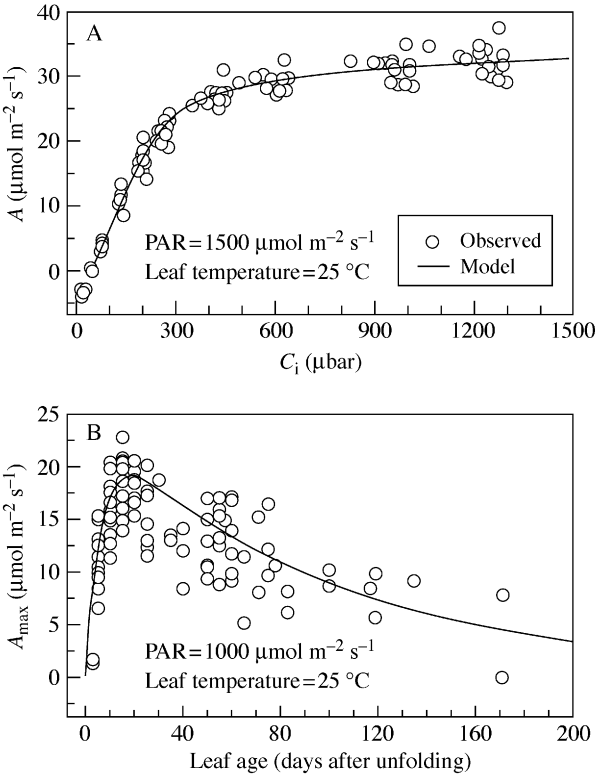

FIG. 2. Photosynthesis sub-model calibration. A, A/C_i response. Solid line represents the prediction of photosynthesis sub-model using measured C_i. B, Leaf age response of A_{max}. Solid line represents the prediction of leaf age function.

Additional measurements used in the model validation were made using the LI-6400 photosynthesis system between February and May 2001. These measurements were made under conditions that differed from the calibration conditions: A/C_i response at 70 and 200 μmol m^{-2} s^{-1} PAR; temperature response at 200 μmol m^{-2} s^{-1} PAR at three different CO_2 levels (200, 370 and 1200 μmol mol^{-1}); and light responses of leaves of different ages (8, 30, 68 and 180 d after unfolding). Other measurement conditions (e.g. automated protocol criteria) remained the same.

Model calibration and validation

Rather than fitting all parameters simultaneously, stepwise calibration of individual components of the model was performed so that each component of the model could be updated independently as needed. That is, the photosynthetic parameters (V_{cm25}, J_{m25}, R_{d25}) were first determined by fitting the biochemical model of photosynthesis (Farquhar *et al.*, 1980) to the A/C_i response using measured C_i at controlled steady-state conditions where PAR was fixed at 1500 μmol m^{-2} s^{-1}, relative humidity was around 50 %, and leaf temperature was controlled at 25 °C (Fig 2A). In addition, V_{cmax} and J_{max} were estimated for individual leaves over a range of temperatures. Temperature depen-

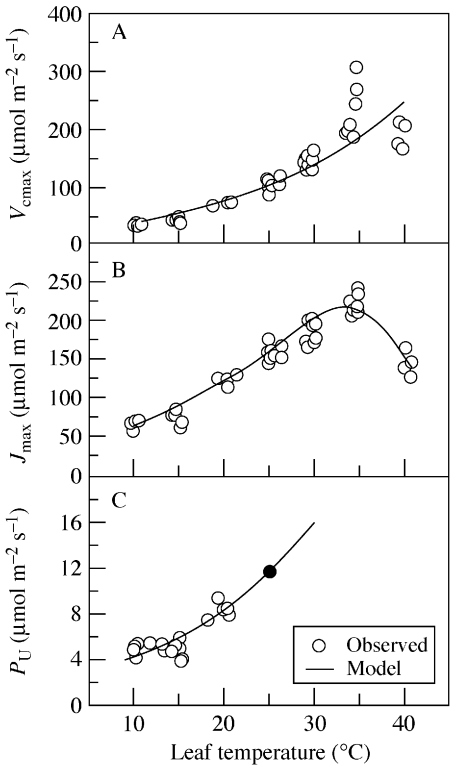

FIG. 3. Temperature dependence determination of photosynthesis sub-model. A, Rubisco capacity (V_{cmax}). B, Potential rate of electron transport (J_{max}). C, Triose phosphate utilization rate (P_u). Closed circle indicates the extrapolated P_{u25}.

dence of V_{cmax} and J_{max} was then determined by fitting eqns (A7) and (A8) with these estimates, respectively (Fig. 3). Temperature dependence of P_u was determined by fitting eqn (A7) with the net photosynthesis data collected between 10 and 20 °C at 1500 μmol mol^{-1} CO_2 and 1500 μmol m^{-2} s^{-1} PAR, assuming that A is primarily governed by the rate of TPU when temperature is low while CO_2 and light are not limiting (Sharkey, 1985). P_{u25} was estimated by extrapolating the resulting equation (Fig. 3C). Temperature dependencies of K_c (Michaelis–Menten constant of Rubisco for CO_2), K_o (Michaelis–Menten constant of Rubisco for O_2), Γ* (mitochondrial respiration in the light) and R_d (CO_2 compensation point in the absence of R_d) were adopted from de Pury and Farquhar (1997), assuming that these parameters were invariant across species. Leaf age dependence, given by eqn (A10), was fitted with the data collected in the 1999 experiment (Fig. 2B). The parameter values of the stomatal conductance model were determined using the gas exchange data collected specifically for calibration of this sub-model. The data included a range of CO_2 concentrations, relative humidity levels, PAR levels and temperatures, while those conditions where A might approach zero were excluded (Collatz *et al*., 1991). Non-linear regression with the Gauss–Newton method was used to estimate the parameter values of the model (Freund and Littell, 1991). No parameter values in the energy balance equation were specifically calibrated in this study. An attempt was also made to calibrate multiple parameters (V_{cmax}, J_{max}, P_u and their temperature dependencies, and R_d) simultaneously by fitting the combined model with the pooled data. As the number of parameters increased, the attempt at fitting the model using a non-linear regression technique failed to obtain a set of converging parameters regardless of the optimization method.

Radiation absorbed by the leaf in the solar and thermal wavebands (R_{abs}) inside the leaf chamber was estimated using the following empirical relation (LI-COR, 1998):

$$R_{abs} = 0{\cdot}5\ \alpha_{LED} k I_0 + \varepsilon\sigma T_w^4 \quad (1)$$

where α_{LED} is the leaf absorptivity (0·84) averaged over the spectrum of the LED light source, k is an empirical conversion factor (0·19) from the incoming PAR level (I_0) in the leaf chamber to total visible and near infrared energy, and T_w is the temperature of the chamber wall. T_w was assumed to be the same as air temperature (T_a) measured inside the leaf chamber.

Other photosynthetic parameters were obtained from de Pury and Farquhar (1997). The combined model was programmed with the computer programming language Pascal (Source code available from the authors upon request).

Linear regression of the model prediction on the observed values was used to evaluate the model performance. Significance of the linear regression, slope unity and zero intercept were tested. Bias and root mean square error (RMSE) were also evaluated as measures of model performance (Retta *et al*., 1991).

RESULTS

Calibration of the sub-models

A/C_i response of rose leaves, examined at a PAR of 1500 μmol m^{-2} s^{-1} and leaf temperature of 25 °C, followed typical A/C_i response patterns of C_3 plants (Fig. 2A). Estimates of the photosynthetic parameters were 102·4 ± 2·04 (approximated standard error), 162·0 ± 2·04 and 1·26 ± 0·289 μmol m^{-2} s^{-1} for V_{c25}, J_{m25} and R_{d25}, respectively. The photosynthesis sub-model described the photosynthetic response very well over a range of measured C_i at 25 °C. The transition from A_c to A_j occurred at C_i = 293 μbar. The limitation due to A_p did not appear to take place under this condition. Photosynthetic rates of young rose leaves increased rapidly up to 20 d after unfolding, then declined gradually as leaves aged (Fig. 2B). The model explained the temperature response of V_{cmax} and J_{max} well (Fig. 3). The BWB model was capable of accounting for 70 % of the observed variation in measured stomatal conductance of calibration data (Fig. 4).

Prediction of A *by the combined model*

Prediction of A by the combined model is represented graphically against calibration data (Fig. 5). At 10 °C, A was insensitive to high CO_2 levels. The combined model simulated this observed pattern well; that is, a linear

increase up to the ambient level of CO_2, followed by a flat line as CO_2 increased further (Fig. 5A). The model predicted a flat response at high CO_2 levels as a result of a limitation due to A_p. At 10 °C, the model predicted a nearly direct transition from the A_c- (linear increase) to the A_p-limited (flat response) region, with a brief period of A_j limitation (170–230 μbar of C_i) between the two regions. At 20 °C, the model behaved such that the transition from A_c to A_j occurred around 250 μbar and the transition between A_j and A_p took place around 700 μbar (Fig. 5A). At 30 °C, the limitation due to A_p was not realized at high CO_2 concentrations (up to 1500 μbar), while the transition from A_c to A_j occurred at 320 μbar (Fig. 5B). At 40 °C, the model predicted that A was solely limited by A_j throughout all CO_2 levels (Fig. 5B). The model successfully reproduced the observed pattern of A/C_i responses at all four leaf temperatures.

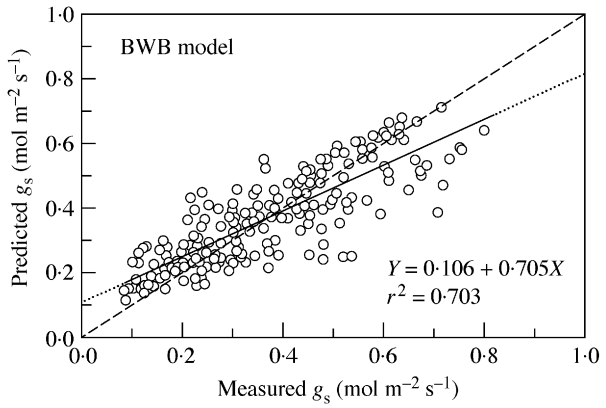

FIG. 4. Linear regression of predicted g_s on measured g_s as a result of BWB model calibration. Dashed line indicates one to one relationship.

The photosynthetic response to leaf temperature was simulated fairly well over the entire range of temperatures at various ambient CO_2 concentrations (Fig. 5C). At C_a = 1200 μbar, the optimal leaf temperature that yielded the maximal net photosynthetic rate of 37·0 μmol m^{-2} s^{-1} was around 32 °C. The optimal temperature decreased with decreasing ambient CO_2 concentrations. Despite the fact that parameters related to the light response were not determined experimentally, the model response to PAR was also simulated fairly well, exhibiting saturation at a net photosynthetic rate of 21·8 μmol m^{-2} s^{-1} when incident PAR was above 1100 μmol m^{-2} s^{-1} and A_c started limiting A (Fig. 5D).

Model validation

The combined model predicted the observed pattern of A/C_i response quite well at both light flux densities (70 and 200 μmol m^{-2} s^{-1}) (Fig. 6A). The model tended to

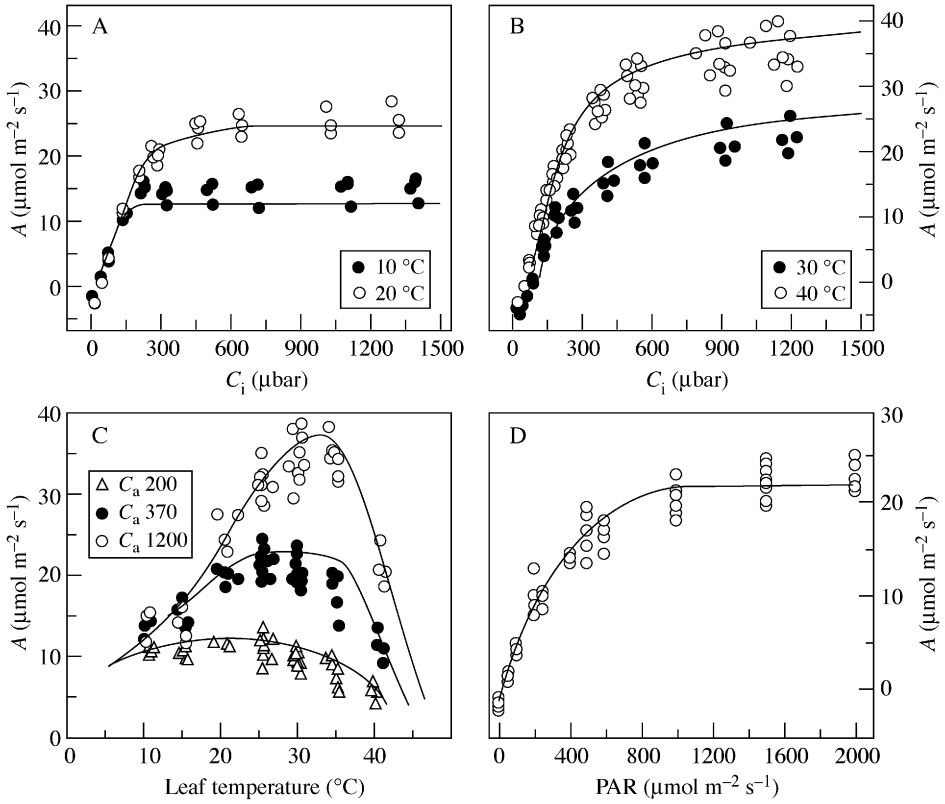

FIG. 5. Prediction of net photosynthesis (A). Lines represent the combined model prediction; symbols are observations of calibration data. A, A/C_i responses at 10 and 20 °C. B, A/C_i responses at 30 and 40 °C. C, Temperature response at three C_a levels (μbar). D, Light response at C_a of 350 μbar at 25 °C. Relative humidity was maintained around 50 %.

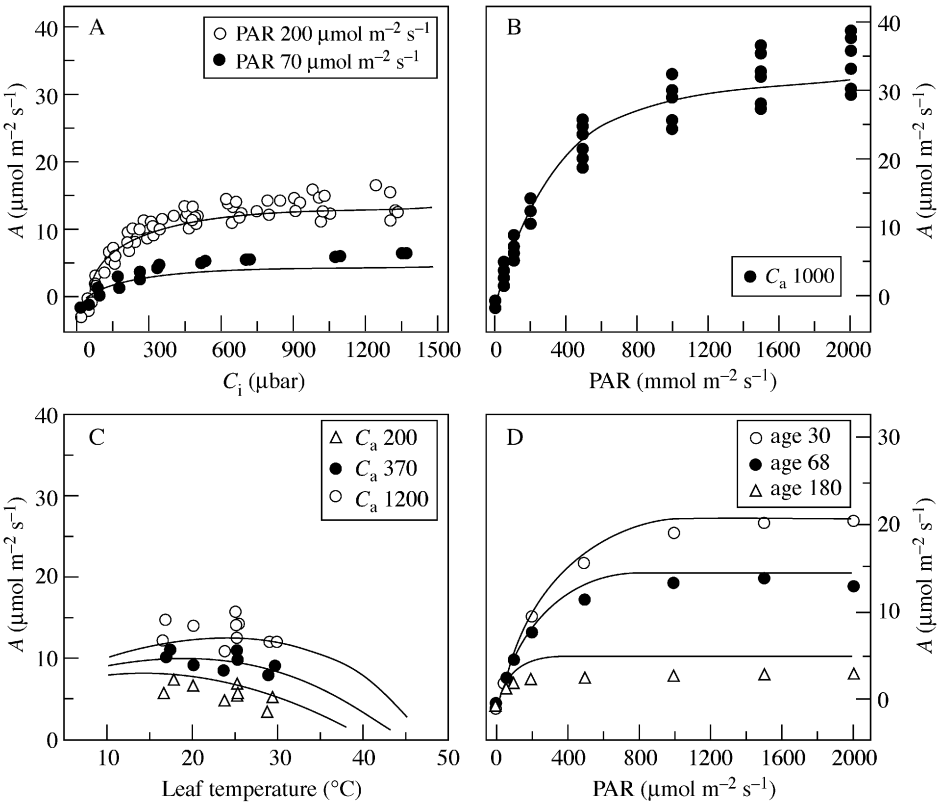

FIG. 6. Validation of the model for net photosynthesis (A). Lines represent the combined model prediction; symbols are observations of validation data. A, A/C_i responses at two incident PAR levels (70 and 200 μmol m^{-2} s^{-1}) at 25 °C. B, Light response at C_a of 1000 μbar at 25 °C. C, Temperature response at three C_a levels under incident PAR of 200 μmol m^{-2} s^{-1}. D, Light response of leaves of different age (30, 68 and 180 d after unfolding) at ambient CO_2 (350 μbar) at 25 °C. Relative humidity was maintained around 50 %.

underestimate A slightly at high CO_2 concentrations. Light responses at high CO_2 (C_a =1000 μbar) were also investigated (Fig. 6B), and the results from the model agreed with the observed light response pattern. The model was capable of predicting the observed pattern of temperature responses at three ambient CO_2 concentrations with PAR at 200 μmol m^{-2} s^{-1} (Fig. 6C). The model also predicted the photosynthetic response to PAR at various leaf ages reasonably well (Fig. 6D). For a leaf age of 180 d, the model slightly overestimated A compared with observed values.

Performance of the combined model was evaluated by comparing observed values with predicted values. The regression F-value was significant for all variables listed in Table 1. The regression line slope deviated significantly from unity for all variables but A. The combined model successfully reproduced the observed response in A (r^2 = 0·956). The model tended to underestimate both g_s and E as indicated by negative bias values (Table 1).

TABLE 1. *Performance of the combined model against validation data*

Variable	Intercept	Slope	r^2	Bias	RMSE
A	0·244	1·001	0·956	0·254	1·499
g_s	0·675**	0·526**	0·491	–0·062	0·127
E	1·011**	0·505**	0·473	–0·775	1·500
C_i	–2·477	1·066**	0·931	27·53	103·2
T_L	–2·602**	1·094**	0·976	–0·361	0·715

Shown are values for intercepts, slopes, r^2, bias and root mean square error (RMSE) for linear regressions of model prediction (Y) on observed values (X) for net photosynthetic rates (A), stomatal conductance (g_s), transpiration (E), intercellular CO_2 partial pressure (C_i) and leaf temperature (T_L).

Number of observations = 170.

** Significantly different from intercept = 0 and slope = 1 (P < 0·01).

DISCUSSION

Values for V_{cmax} of 102·4 and J_{max} of 162·0 μmol m^{-2} s^{-1} were obtained for young rose leaves ('Kardinal') at 25 °C. Using young leaves of rose 'Sonia', Gonzalez-Real and Baille (2000) reported values of 66 μmol m^{-2} s^{-1} for V_{cmax} and 155·8 μmol m^{-2} s^{-1} for J_{max}. Their J_{max} value agrees reasonably well with present results, whereas their estimate of V_{cmax} is lower than that found here.

Various functions have been used to describe the temperature dependence of V_{cmax} and J_{max}. For example, Harley *et al.* (1992) and Leuning (1995) employed a compound function with an optimum for both V_{cmax} and J_{max}, whereas de Pury and Farquhar (1997) used an exponential growth function (the Arrhenius function) for V_{cmax}. In our parameterization of V_{cmax}, we observed a

slight decline between 35 and 40 °C. However, we opted to use the Arrhenius function to describe the temperature dependence of V_{cmax} because it resulted in better overall performance for typical growing temperatures. In a recent survey, Leuning (2002) reported that functions describing the temperature response of the photosynthetic parameters V_{cmax} and J_{max} at 25 °C show little variation between different species at leaf temperature <30 °C, while above this temperature variation is large and species-dependent. Bernacchi *et al*. (2001) published a set of modified temperature response functions of Rubisco-related parameters that improved predictions of Rubisco-limited A over the temperature range 10–40 °C.

The A/C_i response at low temperature (10 °C) shows that short-term increases of CO_2 did not result in increased photosynthesis (Fig. 5A). We hypothesized that this response was the result of limitation because of TPU, and implemented this in the model following Harley *et al*. (1992). Inclusion of the TPU limitation greatly improved the model prediction of response to high CO_2 at low temperature. Implementation of the TPU limitation in the model could be critical, especially for glasshouse crops, including cut-flower roses, because many commercial glasshouses practice CO_2 enrichment during winter. The model could help growers decide whether or not to provide plants with additional CO_2 under unusual temperature and light conditions. Some modellers have introduced smoothing factors for the transition between the limitations, as it appears, in reality, to be more gradual than that predicted by eqn (A1) (Collatz *et al*., 1991; Nikolov *et al*., 1995).

In our model, solutions for C_i and T_L were obtained by numerical methods. In most cases, the number of iterations was kept below ten for both C_i and T_L determinations when the model was tested for a range of environmental situations. A drawback of applying numerical solutions is that they are time- and resource-consuming. In addition, Baldocchi (1994) reported that iterative solutions for A become unstable when g_b and Γ^* exceed critical values. While some modellers (Collatz *et al*., 1991; Harley *et al*., 1992) have used iterative solutions to couple photosynthesis–stomatal conductance models, others have successfully yielded analytical solutions for coupling processes so as to reduce the load of the iterations (Baldocchi, 1994; Nikolov *et al*., 1995; Wang and Leuning, 1998). Linking the processes through analytical solutions could speed up the model execution when used in extensive simulation tasks (e.g. simulation of monthly or annual canopy productivity for various environmental scenarios).

While the combined model yielded very good estimation of net photosynthesis, it failed to achieve high accuracy in predicting g_s and E. There was considerable variation in estimation of g_s that was not explained by the coupled model (Table 1; $r^2 = 0{\cdot}491$). The light and A/C_i response measurements in this study were made using the automated protocol built into the photosynthesis system (LI-6400). Despite the fact that fairly conservative criteria were used to advance to the next step after leaves had equilibrated to the initial condition, it is possible that second or later readings in the measurement series were taken before the stomata were fully acclimated to the new environment. Therefore, the performance of the model was also tested using only the first readings from each automated measurement series, since these readings were taken when leaves were equilibrated to the initial conditions. The test revealed that the model performed slightly better against the first readings than against all readings for predicting g_s and E. That is, the slope of linear regression for E (= 0·881) was not different from unity. The r^2-values for both g_s and E were also improved. However, the slope for g_s (= 0·651) was still significantly different from unity at $P < 0{\cdot}01$ (Table 2). This indicates that some measurements might have been made before leaves entered steady state, and this could account, in part, for the discrepancy in performance of the model for g_s and E when tested against all readings of validation data. This suggests that when data are to be used for calibration and validation of stomatal conductance models, gas exchange measurements using an automated protocol built into a photosynthesis system should be made with prolonged equilibration times. Leaves in the canopy are more likely to be exposed to dynamic changes of multiple environmental factors than to stay in steady state. A dynamic model rather than a steady-state model would be of more use for predicting stomatal conductance in dynamically changing environments. Models for dynamic stomatal responses to changing light regimes (Pearcy *et al*., 1997) and humidity (Jarvis *et al*., 1999) have been introduced.

TABLE 2. *Performance of the combined model against only the first readings of automated measurements using LI-6400 in validation data*

Variable	Intercept	Slope	r^2	Bias	RMSE
A	0·826	0·960	0·952	0·080	2·239
g_s	0·048	0·651**	0·591	–0·099	0·135
E	–0·148	0·881	0·648	–0·757	1·411
C_i	18·52	0·956*	0·986	–2·567	28·12
T_L	–1·990	1·090*	0·962	0·265	0·901

Shown are values for intercepts, slopes, r^2, bias and root mean square error (RMSE) for linear regressions of model prediction (Y) on observed values (X) for net photosynthetic rates (A), stomatal conductance (g_s), transpiration (E), intercellular CO_2 partial pressure (C_i) and leaf temperature (T_L).

Number of observations = 33.

*, **, Significantly different from intercept = 0 and slope = 1 at $P < 0{\cdot}05$ and $P < 0{\cdot}01$, respectively.

In modelling stomatal conductance there is no consensus such as for the FvCB model in photosynthesis, and available models are basically empirical. Two main approaches have commonly been used in modelling stomatal conductance. The first, proposed by Jarvis (1976), is based on empirical stomatal responses to environmental conditions, such as radiation, vapour pressure deficit (VPD), temperature, soil water potential and CO_2 concentration. The second commonly used approach is based on the observed link between stomatal conductance and photosynthesis (Wong *et al*., 1979). Ball *et al*. (1987) implemented this relation to model stomatal conductance as a function of CO_2 concentration,

relative humidity at the leaf surface (h_s) and net photosynthesis. Lack of a mechanistic basis for using h_s in the stomatal conductance model was criticized, and it was suggested that h_s be replaced by VPD (Aphalo and Jarvis, 1991; Lloyd, 1991). Leuning (1995) modified the BWB model by replacing h_s with VPD at the leaf surface (D_s) to allow for low intercellular CO_2 concentrations by using $(C_s - \Gamma)$ in the denominator so that the data when $A \rightarrow 0$ could be included. We also tested a coupled model incorporating the Leuning model for rose leaves and found that it performed similarly to the BWB model (data not shown; see Kim, 2001 for details). BWB-type models (including the Leuning model) have been widely used because of their simplicity and plasticity in linking leaf photosynthesis to stomatal conductance (Collatz *et al*., 1991; Harley *et al*., 1992; Nikolov *et al*., 1995). The benefit of including the BWB model in a coupled model is that its variables can be determined from mechanistic photosynthesis and energy balance models (Baldocchi, 1994). It is also advantageous because stomatal responses to various factors can be realized indirectly through their effects on photosynthesis since the model operates as a function of A.

The present model is to be extended to include water- and nutrient-related variables of both the root-zone and plant. The effect of soil and plant water status might be implemented through regulating the slope coefficient (m) in the stomatal model as a function of leaf water potential. Van Wijk *et al*. (2000) examined the applicability of the commonly used stomatal conductance models when a soil water stress function was incorporated. They reported that the slope coefficient of the BWB model was related to both air temperature and soil water content, while the Leuning- and Jarvis-type models showed a relationship only with soil water content. Thus, Van Wijk *et al*. (2000) concluded that the models incorporating VPD other than h_s would be better suited for their study. Leaf nitrogen content can also be linked to photosynthetic parameters (Leuning *et al*., 1995; Gonzalez-Real and Baille, 2000). To date, information on the effect of other macro- and micronutrients on the gas exchange characteristics of leaves is not as complete as that for nitrogen.

In conclusion, the present coupled gas exchange model for a rose leaf is capable of predicting photosynthesis, intercellular CO_2 concentration and leaf temperature as a function of radiation, air temperature, ambient CO_2, leaf age and relative humidity, but predictions of stomatal conductance and transpiration are less satisfactory. The model has simple input and output structures and can be used as a module in a crop simulation model. As a stand-alone application the model can assist rose growers making glasshouse environmental control decisions.

ACKNOWLEDGEMENTS

This research was supported in part by a grant from the Joseph Hill Foundation. We thank Dr M. Parrella for use of the photosynthesis system, and Drs L. Oki, J. Baker and G. McMaster for helpful comments on the manuscript.

LITERATURE CITED

Aphalo PJ, Jarvis PG. 1991. Do stomata respond to relative humidity? *Plant, Cell and Environment* **14**: 127–132.

Baldocchi D. 1994. An analytical solution for coupled leaf photosynthesis and stomatal conductance models. *Tree Physiology* **14**: 1069–1079.

Ball JT, Woodrow IE, Berry JA. 1987. A model predicting stomatal conductance and its contribution to the control of photosynthesis under different environmental conditions. In: Biggens J, ed. *Progress in photosynthesis research*. The Netherlands: Martinus Nijhoff Publishers.

Bernacchi CJ, Singsaas EL, Pimentel C, Portis ARJ, Long SP. 2001. Improved temperature response functions for models of Rubisco-limited photosynthesis. *Plant, Cell and Environment* **24**: 253–259.

Campbell GS, Norman JM. 1998. *Introduction to environmental biophysics. 2nd edn*. New York: Springer.

Cannell MGR, Thornley JHM. 1998. Temperature and CO_2 responses of leaf and canopy photosynthesis: a clarification using the non-rectangular hyperbola model of photosynthesis. *Annals of Botany* **82**: 883–892.

Collatz GJ, Ball JT, Grivet C, Berry JA. 1991. Physiological and environmental regulation of stomatal conductance, photosynthesis and transpiration: a model that includes a laminar boundary layer. *Agricultural and Forest Meteorology* **54**: 107–136.

de Pury DGG, Farquhar GD. 1997. Simple scaling of photosynthesis from leaves to canopies without the errors of big-leaf models. *Plant, Cell and Environment* **20**: 537–557.

Farquhar GD, von Caemmerer S, Berry JA. 1980. A biochemical model of photosynthetic CO_2 assimilation in leaves of C_3 species. *Planta* **149**: 78–90.

Freund RJ, Littell RC. 1991. *SAS system for regression*. Cary, NC: SAS Institute Inc.

Gonzalez-Real MM, Baille A. 2000. Changes in leaf photosynthetic parameters with leaf position and nitrogen content within a rose plant canopy (*Rosa hybrida*). *Plant, Cell and Environment* **23**: 351–363.

Harley PC, Thomas RB, Reynolds JF, Strain BR. 1992. Modelling photosynthesis of cotton grown in elevated CO_2. *Plant, Cell and Environment* **15**: 271–282.

Jarvis AJ, Young PC, Taylor CJ, Davies WJ. 1999. An analysis of the dynamic response of stomatal conductance to a reduction in humidity over leaves of *Cedrella odorata*. *Plant, Cell and Environment* **22**: 913–924.

Kim S-H. 2001. *Photosynthesis models and canopy management optimization in cut-flower roses*. PhD Thesis. University of California, Davis, USA.

Leuning R. 1995. A critical appraisal of a combined stomatal-photosynthesis model for C_3 plants. *Plant, Cell and Environment* **18**: 339–355.

Leuning R. 2002. Temperature dependence of two parameters in a photosynthesis model. *Plant, Cell and Environment* **25**: 1205–1210.

Leuning R, Kelliher FM, de Pury DGG, Schulze E-D. 1995. Leaf nitrogen, photosynthesis, conductance and transpiration: scaling from leaves to canopies. *Plant, Cell and Environment* **18**: 1183–1200.

LI-COR. 1998. *Using the LI-6400: Portable photosynthesis system. 2nd edn*. Lincoln, NE: LI-COR, Inc.

Lieth JH, Pasian CC. 1990. A model for net photosynthesis of rose leaves as a function of photosynthetically active radiation, leaf temperature, and leaf age. *Journal of the American Society for Horticutural Science* **115**: 486–491.

Lloyd J. 1991. Modelling stomatal responses to environment in *Macadamia integrifolia*. *Australian Journal of Plant Physiology* **18**: 649–660.

Medlyn BE, Badeck FW, de Pury DGG, Barton CVM, Broadmeadow M, Ceulemans R, De Angelis P, Forstreuter M, Jach ME, Kellomaki S *et al*. 1999. Effects of elevated CO_2 on photosynthesis in European forest species: a meta-analysis of model parameters. *Plant, Cell and Environment* **22**: 1475–1495.

Nikolov NT, Massman WJ, Shoettle AW. 1995. Coupling biochemical and biophysical processes at the leaf level: an equilibrium photosynthesis model for leaves of C_3 plants. *Ecological Modelling* **80**: 205–235.

Oki LR, Lieth JH, Tjosvold SA. 2001. Irrigation of *Rosa hybrida* L.

'Kardinal' based on soil moisture tension increases productivity and flower quality. *Acta Horticulturae* **547**: 213–219.

Pearcy RW, Gross LJ, He D. 1997. An improved dynamic model of photosynthesis for estimation of carbon gain in sunfleck light regimes. *Plant, Cell and Environment* **20**: 411–424.

Retta A, Vanderlip RL, Higgins RA, Moshier LJ, Feyerherm AM. 1991. Suitability of corn growth models for incorporation of weed and insect stresses. *Agronomy Journal* **83**: 757–765.

Sharkey TD. 1985. Photosynthesis in intact leaves of C_3 plants: physics, physiology and rate limitations. *Botanical Review* **51**: 53–105.

Van Wijk MT, Dekker SC, Bouten W, Bosveld FC, Kohsiek W, Kramer K, Mohren GMJ. 2000. Modeling daily gas exchange of a Douglas-fir forest: comparison of three stomatal conductance models with and without a soil water stress function. *Tree Physiology* **20**: 115–122.

Wang YP, Leuning R. 1998. A two-leaf model for canopy conductance, photosynthesis and partitioning of available energy. I: Model description and comparison with a multi-layered model. *Agricultural and Forest Meteorology* **91**: 89–111.

Wong SC, Cowan IR, Farquhar GD. 1979. Leaf conductance in relation to rate of CO_2 assimilation. *Plant Physiology* **78**: 821–825.

Wullschleger SD. 1993. Biochemical limitation to carbon assimilation in C_3 plants - A retrospective analysis of the A/C_i curves from 109 species. *Journal of Experimental Botany* **44**: 907–920.

APPENDIX

TABLE A1. *Equations of the photosynthesis, stomatal conductance, and energy balance models*

Equation	Description	No.
Photosynthesis model (FvCB model)		
$A = V_c - 0{\cdot}5V_0 - R_d = \min\{A_c, A_j, A_p\} - R_d$	Net photosynthetic rate	(A1)
$A_c = V_{c\,max}\dfrac{C_i - \Gamma*}{C_i + K_c(1 + O/K_o)}$	Rubisco-limited photosynthetic rate	(A2)
$A_j = \dfrac{J(C_i - \Gamma*)}{4(C_i + 2\Gamma*)}$	RuBP regeneration limited photosynthetic rate through electron transport	(A3)
$\theta J^2 - (I_2 + J_{max})J + I_2 J_{max} = 0$	Light dependence of the rate of electron transport	(A4)
$I_2 = I(1 - f)(1 - \delta)/2$	PAR effectively absorbed by Photosystem II	(A5)
$A_p = 3P_u$	TPU limited photosynthetic rate	(A6)
$K_T = k_{25}\exp[E_a(T_L - 25)/\{298R(T_L + 273)\}]$	Arrhenius function; temperature dependence of K_c, K_o, R_d, V_{cmax} and P_u	(A7)
$J_{max} = J_{m\,25}\exp\left[\dfrac{(T_L - 25)E_a}{R(T_L + 273)298}\right] \dfrac{\left[1 + \exp\left(\dfrac{S298 - H}{R298}\right)\right]}{\left[1 + \exp\left(\dfrac{S(T_L + 273) - H}{R(T_L + 273)}\right)\right]}$	Temperature dependence of J_{max}	(A8)
$\Gamma* = 36{\cdot}9 + 1{\cdot}88(T_L - 25) + 0{\cdot}036(T_L - 25)^2$	Temperature dependence of $\Gamma*$	(A9)
$f(\xi) = d_0(1 - \exp(-d_1\xi))\exp(-d_2\xi)$	Leaf age dependence of J_{max}, V_{cmax} and P_u	(A10)
Stomatal conductance model (BWB model)		
$g_s = b + mA\dfrac{h_s}{(C_s/P_a)}$	Stomatal conductance	(A11)
$\Gamma = \dfrac{R_d(K_c(1 + O/K_o)) + V_{c\,max}\Gamma*}{V_{c\,max} - R_d}$	CO_2 compensation point in the presence of R_d	(A12)
$C_s = C_a - A\dfrac{1{\cdot}37}{g_b}P_a$	Estimation of CO_2 partial pressure at the leaf surface	(A13)
$g_b = 0{\cdot}147\sqrt{\dfrac{u}{d}}$	Boundary layer conductance in relation to wind speed (u) and leaf dimension (d)	(A14)
$d = 0{\cdot}72w$	Characteristic dimension of a leaflet in relation to width (w)	(A15)
$a_h h_s^2 + b_h h_s + c_h = 0$ where $\begin{cases} a_h = (g_1 A)/C_s \\ b_h = g_0 + g_b - (g_1 A/C_s) \\ c_h = (-h_a g_b) - g_0 \end{cases}$	Quadratic equation to obtain h_s by combining g_s with diffusion equation	(A16)
$D_s = (1 - h_s)e_s$	Vapour pressure deficit at the leaf surface	(A17)
Energy balance model		
$T_L = T_a + \dfrac{R_{abs} - \varepsilon\sigma T_a{}^4 - \lambda g_v D/P_a}{c_p(g_h + g_r) + \lambda((de_s(T_a)/dT)/P_a)g_v}$	Linear solution of the energy budget equation for T_L	(A18)
$g_v = 0{\cdot}5\dfrac{g_s g_b}{g_s + g_b}$	Total water vapour conductance per surface leaf area	(A19)
$g_h = \dfrac{0{\cdot}135}{0{\cdot}147}g_b$	Heat conductance for the boundary layer	(A20)
$g_r = \dfrac{4\varepsilon\sigma T_L^3}{C_p}$	Radiative conductance	(A21)
$e_s(T) = 0{\cdot}611\exp\left(\dfrac{17{\cdot}502T}{240{\cdot}97 + T}\right)$	Saturated water vapour pressure at temperature T	(A22)
$E = 2g_v\left(\dfrac{e_s(T_L) - e_a}{P_a}\right)$	Transpiration rate	(A23)
$C_i = C_a - A\left(\dfrac{1{\cdot}6}{g_s} + \dfrac{1{\cdot}37}{g_b}\right)P_a$	Obtaining C_i by coupling A and g_s	(A24)

TABLE A2. *Variables, parameters, and their values used in the model*

Symbol	Value	Units	Description	
Photosynthesis model				
Γ	–	μbar	CO_2 compensation point in the presence of R_d	
Γ^*	–	μbar	CO_2 compensation point in the absence of R_d	
ξ	–	day	Leaf age counted as days after unfolding	
θ	0·7[a]	–	Curvature of response of electron transport to PAR	
δ	0·15	–	Leaf reflectance plus transmittance	
A	–	μmol m^{-2} s^{-1}	Net photosynthetic rate	
A_c	–	μmol m^{-2} s^{-1}	Rubisco-limited CO_2 assimilation rate	
A_j	–	μmol m^{-2} s^{-1}	Electron transport-limited CO_2 assimilation rate	
A_{max}	–	μmol m^{-2} s^{-1}	Light-saturated A at ambient $[CO_2]$	
A_p	–	μmol m^{-2} s^{-1}	Triose phosphate utilization-limited CO_2 assimilation rate	
C_i	–	μbar	Intercellular CO_2 partial pressure	
d_0	1·296	–	Scaling factor of leaf age effect	
d_1	0·1468	–	Empirical coefficient to determine growth of leaf age effect	
d_2	0·0103	–	Empirical coefficient to determine downward slope of leaf age effect	
E_a	–	kJ mol^{-1}	Activation energy	
f	0·15[a]	–	Spectral correction factor	
H	219·4	kJ mol–1	Curvature parameter of the temperature dependence J_{max}	
I	–	μmol quanta m^{-2} s^{-1}	Incident PAR	
J	–	μmol electrons m^{-2} s^{-1}	Electron transport rate	
J_{m25}	162·0	μmol m^{-2} s^{-1}	Potential rate of electron transport at 25 °C	
K_{c25}	404[a]	μbar	Michaelis–Menten constant of Rubisco for CO_2	
K_{o25}	248[a]	mbar	Michaelis–Menten constant of Rubisco for O_2	
O	205[a]	mbar	Oxygen partial pressure	
P_{u25}	11·55	μmol m^{-2} s^{-1}	Rate of triose phosphate utilization at 25 °C	
R	8·314	J mol^{-1} K^{-1}	Universal gas constant	
R_{d25}	1·260	μmol m^{-2} s^{-1}	Mitochondrial respiration in the light at 25 °C	
S	704·2	J mol^{-1} K^{-1}	Electron transport temperature response parameter	
T_L	–	°C	Leaf temperature	
V_c	–	μmol m^{-2} s^{-1}	Carboxylation rate	
V_{cm25}	102·4	μmol m^{-2} s^{-1}	Photosynthetic Rubisco capacity at 25 °C	
V_o	–	μmol m^{-2} s^{-1}	Oxygenation rate	
Variables with temperature dependence				E_a
J_{max}	–	μmol m^{-2} s^{-1}	Maximum rate of electron transport	43·3
K_c	–	μmol m^{-2} s^{-1}	Michaelis–Menten constant of Rubisco for CO_2	59·4[a]
K_o	–	μmol m^{-2} s^{-1}	Michaelis–Menten constant of Rubisco for O_2	36·0[a]
P_u	–	μmol m^{-2} s^{-1}	Triose phosphate utilization rate	47·1
R_d	–	μmol m^{-2} s^{-1}	Mitochondrial respiration in the light	66·4[a]
V_{cmax}	–	μmol m^{-2} s^{-1}	Maximum rate of rubisco carboxylation	45·5
Stomatal conductance model				
b	0·0960	mol m^{-1} s^{-1}	Minimum stomatal conductance to water vapour at the light compensation point in the BWB model	
C_a	–	μbar	Ambient CO_2 partial pressure	
C_s	–	μbar	CO_2 partial pressure at the leaf surface	
g_b	–	mol m^{-2} s^{-1}	Boundary layer conductance to water vapour	
g_s	–	mol m^{-2} s^{-1}	Stomatal conductance to water vapour	
h_a	–	–	Relative humidity of the ambient air	
h_s	–	–	Relative humidity at the leaf surface	
m	10·055	–	Empirical coefficient for the sensitivity of g_s to A, C_s and h_s in the BWB model	
Energy balance model				
ε	0·97	–	Leaf thermal emissivity	
σ	$5{\cdot}67 \times 10^{-8}$	W m^{-2} K^{-4}	Stefan–Boltzmann constant per surface area	
λ	44·0	kJ mol^{-1}	Latent heat of vaporization at 25 °C	
c_p	29·3	J mol^{-1} C^{-1}	Specific heat of air	
D	–	kPa	Vapour pressure deficit of the ambient air	
D_s	–	kPa	Vapour pressure deficit at the leaf surface	
E	–	mol m^{-2} s^{-1}	Transpiration rate per projected leaf area	
e_a	–	kPa	Vapour pressure in the ambient air	
e_s	–	kPa	Vapour pressure at the leaf surface	
g_h	–	mol m^{-2} s^{-1}	Heat conductance for boundary layer per surface leaf area	
g_r	–	mol m^{-2} s^{-1}	Radiative conductance per surface leaf area	
g_v	–	mol m^{-2} s^{-1}	Total water vapour conductance per surface leaf area	
P_a	–	kPa	Atmospheric pressure	
R_{abs}	–	W m^{-2}	Absorbed long-wave and short-wave radiation per surface leaf area	
T_a	–	°C	Air temperature	

Values followed by superscript 'a' are from de Pury and Farquhar (1997). All parameters are projected leaf area basis unless stated otherwise.